Meas. Sci. Technol. **24** (2013) 085302 (8pp) doi:10.1088/0957-0233/24/8/085302

Investigation of nonlinear effects in constant-temperature anemometers

Julien Weiss[1], **Arganthaël Berson**[2] **and Geneviève Comte-Bellot**[3]

[1] Laboratoire de Thermo-Fluide pour le Transport, École de technologie supérieure, 1100 Notre-Dame Ouest, Montréal, Québec H3C 1K3, Canada
[2] School of Engineering and Computing Sciences, University of Durham, South Road, Durham DH1 3LE, UK
[3] Laboratoire de Mécanique des Fluides et d'Acoustique, UMR CNRS 5509, École Centrale de Lyon, 36 avenue Guy de Collongue, F-69134 Ecully Cedex, France

E-mail: julien.weiss@etsmtl.ca

Received 1 May 2013, in final form 29 May 2013
Published 5 July 2013
Online at stacks.iop.org/MST/24/085302

Abstract
The nonlinear behavior of constant-temperature anemometers is investigated experimentally and numerically for three commercially available anemometers. The experiments are performed in the potential core of a subsonic jet by injecting electrical signals of varying amplitudes and frequencies in the hot wire and recording the anemometer output signals. The numerical model is based on Freymuth's theoretical analysis (1977 *J. Phys. E: Sci. Instrum.* **10** 705–10). The two approaches are in good agreement, which demonstrates the validity of Freymuth's nonlinear theory of constant-temperature anemometers. The results confirm that significant errors are made in the third-order turbulence moment, also called the skewness factor, when the amplitude of velocity fluctuations is large and their frequency is not small compared to the cut-off frequency of the system.

Keywords: hot-wire anemometry, turbulence

1. Introduction

The vast majority of data-processing methods used with hot-wire anemometers rely on the 'small-perturbation' approach in which governing equations are linearized around an average operating point. This approach requires that the flow fluctuations remain fairly small compared to their mean value. In this case, well-developed procedures exist, which use either theoretical sensitivity coefficients or direct calibration methods [1].

When large-amplitude fluctuations are present, the small-perturbation hypothesis breaks down, which leads to errors in the interpretation of hot-wire data if nonlinear effects are not taken into account. These errors can be classified in two main categories: (1) errors caused by difficulties in relating the effective cooling velocity sensed by the hot wire to the three components of velocity fluctuations in the flow and (2) errors caused by the thermal inertia of the wire, which introduces parametric excitation in the equations governing the anemometer's output voltage. The first category of errors has been analyzed by, among others, Hinze [2] and Bruun [3], and is caused by the truncation of the series expansion relating the effective cooling velocity sensed by the hot wire to the three components of velocity fluctuations in the flow. This paper is concerned with the second category of errors, which has received considerably less attention in the literature.

A hot wire experiences thermal inertia, which means that it does not respond to a change in excitation instantaneously but with some thermal lag. For small perturbations, when the wire is operated within a constant-current anemometer (CCA) or a constant-voltage anemometer (CVA), the wire behaves as a first-order system, i.e., it can be satisfactorily described by a first-order linear ordinary differential equation (ODE), with a time constant that depends on the type of anemometer [1]. For large velocity fluctuations, however, the wire thermal inertia leads to a first-order ODE with time-dependent coefficients. As a result, the system experiences parametric excitation and higher harmonics are generated in the output signal [1].

Corrsin [4] demonstrated the appearance of higher harmonics in the case of a CCA by using sinusoidal perturbations and the Fourier series. Later on, Comte-Bellot

and Schon [5] extended the analysis to random fluctuations using an analogue computer. They showed that although the higher harmonics created by parametric excitation have a low energy content, they affect odd moments, especially the third moment, also called the skewness factor, because of cross-products between the fundamental and the harmonic contributions. Berson *et al* [6] analyzed the nonlinear response of a CVA by numerically solving its governing equations. They demonstrated the appearance of higher harmonics and their influence on the skewness factor of a turbulent signal extracted from the large eddy simulation of a high-speed jet. Berson *et al* [6] also devised a post-processing method to eliminate all nonlinear effects caused by parametric excitation. To date, this is the only existing procedure that allows the accurate measurement of the third-order turbulence moment with a hot-wire anemometer when large fluctuations are present.

The small-perturbation analysis of constant-temperature anemometer (CTA) circuits has been the subject of many, often contradictory, investigations (e.g. [3] and references therein). The current consensus is that a third-order linear control theory is both necessary and sufficient to describe the behavior of a well-tuned CTA circuit within the small-perturbation hypothesis [7, 8]. Freymuth [9] demonstrated that a typical CTA is governed by three equations: the (nonlinear) bridge imbalance voltage in terms of resistive, inductive and capacitive components included in the circuit, the (linear) characteristics of the feedback amplifier and the (nonlinear) heat-transfer law of the wire including the effect of its thermal inertia. For small perturbations, Freymuth [9] linearized these equations and showed that they are equivalent to one linear third-order ODE that characterizes the frequency response of the CTA.

The effects of large-amplitude velocity fluctuations on the output signal of a CTA have been mainly investigated by Freymuth [10, 11], although some useful results were also obtained by Perry [12]. In the case of large fluctuations, Freymuth recast the three governing equations into one third-order nonlinear ODE and solved it within the approximation of a second-order series expansion. For a sinusoidal velocity perturbation of 50% of the mean, Freymuth demonstrated that a typical CTA circuit generates a second harmonic with amplitude up to 15% of the fundamental at half the cut-off frequency, which in turn generates a skewness factor of about 0.30 instead of zero. Recently, Weiss *et al* [13] resolved the three governing equations of a CTA using the Runge–Kutta method and confirmed Freymuth's analytical results. For example, Weiss *et al* [13] demonstrated that for a turbulence level u'/U of 20%, the error in the skewness factor is lower than 0.01 for frequencies below 10% of the anemometer's cut-off. However, the error increases rapidly when either the amplitude or the frequency of flow fluctuations increases. As shown in [13], the error in the skewness factor is 0.1 either in the case of $u'/U = 20\%$ at 50% of the anemometer's cut-off or in the case of $u'/U = 50\%$ at 25% of the anemometer's cut-off. Moreover, by analyzing turbulent signals extracted from the same large eddy simulation as used by Berson *et al* [6], Weiss *et al* demonstrated that the nonlinearity of their CTA model overestimated the skewness factor of the high-speed jet by about 0.1 at a turbulence level of only 12%. In this example, the turbulent spectra extended up to the cut-off frequency of the CTA, which was about 100 kHz.

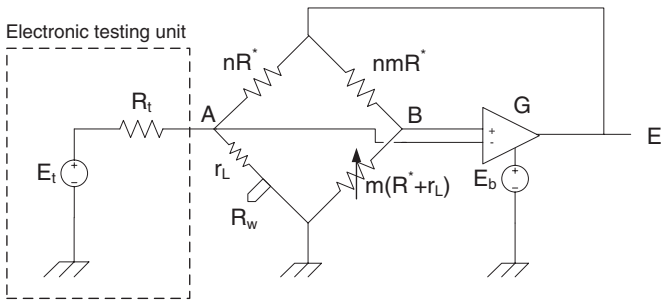

Figure 1. Schematic diagram of a CTA.

One of the conclusions of the aforementioned references is that nonlinear effects can safely be ignored when the CTA cut-off frequency is much higher than the frequencies of the flow fluctuations. A properly tuned modern CTA can reach a frequency response of several tens of kilohertz, which means that most low-speed applications are probably exempt from errors caused by parametric excitation in the circuit. On the other hand, for measurements in high-speed compressible flows, the frequency of flow fluctuations is often very close to or even higher than the cut-off frequency of the anemometer [14]. In these situations, large-amplitude fluctuations will generate harmonics in the CTA output signal and cause errors in the measurements of odd moments.

The purpose of this paper is to demonstrate that the nonlinear theory originally developed by Freymuth [11] correctly represents the behavior of commercial CTAs when large fluctuations are present. This is obtained using a combined numerical and experimental approach. The governing circuit equations are presented in section 2 and the experimental methodology that is used to validate them is described in section 3. A comparison between theory and experiments follows in section 4. The paper ends with a discussion about the possibility of correcting for nonlinear effects in section 5.

2. Governing equations of a CTA

The schematic diagram of a typical CTA is presented in figure 1. A hot wire of resistance R_w is placed in a Wheatstone bridge that is maintained in near equilibrium by a feedback amplifier. The wire is connected to the rest of the circuit through a resistance r_L which lumps the resistance of the wire prongs and that of the cable used between the anemometer and the probe. R^* is the hypothetical wire resistance that would correspond to a perfectly balanced bridge. The value of R^* is important in practice as it is used to specify the wire overheat ratio by adjusting the variable resistance in the lower-right arm of the bridge. Moreover, all resistances in a CTA bridge can be expressed in terms of R^*, and we call m the ratio of resistances between the right and left arms and n the ratio of resistances between the top and bottom arms of the bridge.

The electronic testing unit connected to point A of the Wheatstone bridge is composed of a voltage generator in series

with a resistance R_t, which is chosen to be much larger than the wire resistance. This unit is used to inject a fluctuating current into the hot wire in order to test its frequency response. In practice, this is how the ubiquitous 'square-wave test' is performed [3].

The three governing equations of the circuit are modeling the behavior of (1) the Wheatstone bridge, (2) the feedback amplifier and (3) the hot wire itself.

Following Freymuth [9], the equation representing the behavior of the Wheatstone bridge is expressed as follows:

$$\delta = \frac{nR^*(R^* - R_w)}{((n+1)R^* + r_L)(nR^* + R_w + r_L)}E + M_B\frac{\mathrm{d}E}{\mathrm{d}t} - \frac{(R_w + r_L)nR^*}{(nR^* + R_w + r_L)R_t}E_t, \quad (1)$$

where $\delta = V_B - V_A$ is the voltage in the bridge diagonal between points B and A, E is the CTA output voltage and E_t is the voltage of the test signal, which is used only during electronic testing of the CTA unit and not during flow fluctuation measurements. The first and last terms on the right-hand side of equation (1) are obtained by applying Ohm's and Kirchoff's laws on the Wheatstone bridge. The second term on the right-hand side is then added to model the first-order effects of all reactive elements that can be present in the circuit or in the connecting cables through the adjustable time constant M_B. These reactive elements are not shown in figure 1. It should be noted that this equation assumes that higher order effects in the circuit can be neglected in a properly designed and adjusted anemometer [8].

The amplifier equation reads [9]

$$M''\frac{\mathrm{d}^2E}{\mathrm{d}t^2} + M'\frac{\mathrm{d}E}{\mathrm{d}t} + E = G\delta + E_b, \quad (2)$$

where G is the static gain and M' and M'' are the first- and second-order time constants of the feedback amplifier. The adjustable offset voltage E_b is required to ensure a stable unipolar operation. Equation (2) implicitly assumes a second-order amplifier. For systems using a first-order amplifier, modifications of the theory were presented by Freymuth [15].

Finally, the wire equation is [1]

$$\frac{m_w c_w}{\chi R_0}\frac{\mathrm{d}R_w}{\mathrm{d}t} = \frac{R_w}{(nR^* + R_w + r_L)^2}E^2 - (R_w - R_a)f(U), \quad (3)$$

in which m_w is the mass of the wire, c_w is the heat capacity of the material constituting the wire, χ is the wire temperature coefficient of resistance according to the linear law $R_w = R_0[1 + \chi(T_w - T_0)]$ and R_0 is the resistance of the wire at a reference temperature T_0. The function $f(U)$ characterizes the cooling of the wire by the velocity U normal to its axis and R_a is the resistance of the wire when unheated and placed in the flow. When $f(U)$ takes the form $f(U) = A + B\sqrt{U}$, it is referred to as King's law [1]. Possible reactances included in the left arm of the bridge are neglected in equation (3) as their effect is already included in the bridge time constant M_B.

The anemometer frequency response can be tuned by varying the two adjustable parameters M_B and E_b. According to Freymuth [9], a two-parameter optimization is required by the third-order aspect of the governing equations. In practice, different adjustable 'knobs' are provided for different types of CTAs but they all correspond to a two-parameter adjustment [8].

Equations (1)–(3) are a set of three nonlinear ODEs with R_w, E and δ as unknowns. When flow fluctuations are measured, the velocity $U(t)$ is a forcing function and $E_t = 0$. When an electrical test is performed on the circuit, U is kept constant and $E_t(t)$ becomes the forcing function. Hence, in both cases, these equations represent a nonlinear initial value problem that can be solved numerically for R_w, δ and E. In this paper, we use a classical fourth-order Runge–Kutta method (function *ode45* in Matlab).

In a typical experimental situation, the output voltage $E(t)$ is fed into a calibration curve, which is inverted to recover the measured velocity $U_{\mathrm{meas}}(t)$. The calibration curve is usually acquired in a steady flow (potential core of a jet, free-stream of a wind tunnel, or calibration wind tunnel) and therefore corresponds to the response of an ideal wire without thermal inertia. If the CTA were a perfect instrument, the measured velocity would be equal to the actual velocity, that is: $U_{\mathrm{meas}}(t) = U(t)$. In reality, harmonics are created in $E(t)$ because of the nonlinearity of equations (1) and (3). These harmonics subsist when the output voltage is processed with the calibration curve and as a result, $U_{\mathrm{meas}}(t) \neq U(t)$ [11, 13]. It should be emphasized that these errors are jointly caused by the wire thermal inertia and the electronic circuitry. Other potential sources of errors such as spatial averaging or end-conduction effects are not considered in this analysis.

3. Experimental method

We use three types of commercially available CTAs to verify the validity of equations (1)–(3): a DISA (now Dantec Dynamics) 55M10 unit, a Dantec Dynamics StreamLine system and a Dantec Dynamics Mini-CTA system. All anemometers are sequentially tested with the same Dantec Dynamics 55P01 single normal probe. The wire resistance at a temperature of 25.3 °C is $R_0 = 3.20\ \Omega$ and the leads resistance (connecting cable + support + prongs) is $r_L = 1.63\ \Omega$. In operation, the wire overheat is set to 0.8, which corresponds to a resistance $R^* = 5.76\ \Omega$. The wire is placed in the potential core of an isothermal jet at a velocity $U = 10\ \mathrm{m\,s^{-1}}$ and electrical signals are injected in the different anemometers using an Agilent 33220A signal generator that is connected to the left diagonal of the Wheatstone bridge through a resistor $R_t = 993\ \Omega$. The output $E_t(t)$ of the signal generator and the output $E(t)$ of each anemometer are recorded with a National Instruments PXI6123 16-bit data acquisition card at a sampling frequency of 500 kHz (5000 samples per signal).

The following experimental procedure is used sequentially for each anemometer: firstly, a square-wave signal of amplitude $E_t = 25$ mV (50 mV peak to peak) is injected in the bridge diagonal at a frequency of 1 kHz to optimize the CTA circuit using the standard square-wave test procedure (see [3]). The quality of the optimization is then checked thoroughly by plotting the amplitude transfer function of each anemometer. Secondly, sinusoidal signals of varying frequencies and amplitudes are injected in the bridge diagonal and the skewness of the CTA output signal is computed. If the CTA circuit behaved

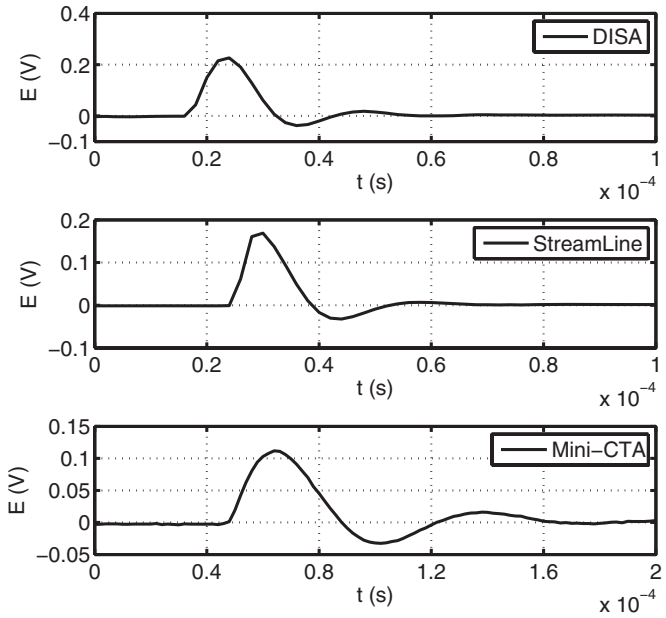

Figure 2. Experimental square-wave responses of the CTAs. Note the different time scales.

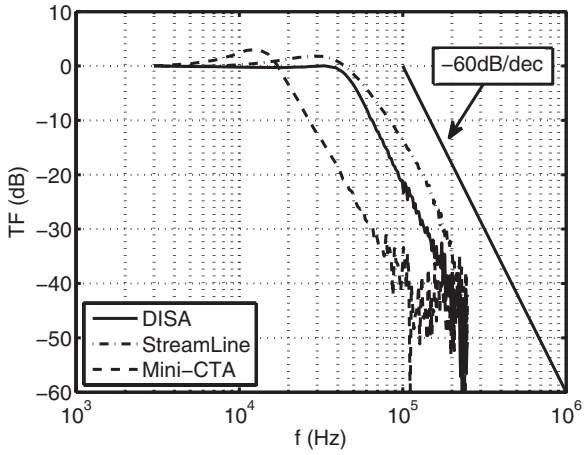

Figure 3. Amplitude transfer function of the CTAs.

linearly, the output skewness would be zero. As will be seen in section 4, this is not the case, implying that the governing equations are indeed nonlinear.

The square-wave responses of the three anemometers are presented in figure 2. They were obtained after careful manual tuning of the adjustable circuit parameters and correspond to the qualitative signal expected for a well-tuned anemometer. From these square-wave signals, the −3 dB cut-off frequency of each anemometer can be obtained using the usual criterion developed by Freymuth [9] and described in Bruun [3]: $f_{\text{cut}} = 1/1.3\tau$, where τ is the width of the pulse. We obtain a cut-off frequency of 50 kHz for the DISA 55M10, 55 kHz for the StreamLine and 20 kHz for the Mini-CTA system.

The amplitude transfer functions, presented in figure 3, are obtained by processing the square-wave output signals using the method developed by Weiss *et al* [14]. The −3 dB cut-off of the transfer functions is generally consistent with the square-wave criterion but there are subtle differences between each transfer function. According to Freymuth [9, 7], a well-tuned CTA is equivalent to a Butterworth filter of order 3, which means that its amplitude transfer function should be flat until the cut-off frequency and should decrease with a −60 dB/decade roll-off above its cut-off. It can be seen from figure 3 that only the DISA 55M10 corresponds to this description. The StreamLine shows a slight increase in its amplitude transfer function before the cut-off and a slope slightly less steep than −60 dB/decade above its roll-off. Similarly, the Mini-CTA system shows a significant increase before its cut-off frequency, although the roll-off itself corresponds to the expected −60 dB/decade slope. It should be noted that a better adjustment of the StreamLine and Mini-CTA systems could not be obtained with the available adjustable circuit parameters. This demonstrates the potential pitfalls of only using the usual square-wave criterion when accurate amplitude transfer functions are required.

4. Comparison between theory and experiments

The chosen procedure to verify the validity of equations (1)–(3) is to inject a known electrical test signal $E_t(t)$ in the Wheatstone bridge using the electronic testing unit and to compare the actual response $E(t)$ of the three anemometers with the output of the numerical model described in section 2. To perform this task, it is first necessary to estimate all the parameters of the governing equations.

4.1. Estimation of circuit parameters

Equations (1)–(3) are a set of three nonlinear ODEs of unknowns $\delta(t)$, $E(t)$ and $R_w(t)$. In the experiments, the velocity $U = 10\ \text{m s}^{-1}$ is a constant and the electronic test signal $E_t(t)$ is the forcing function. The function $f(U)$ is obtained by direct calibration using a Pitot tube as reference. The resistances $r_L = 1.63\ \Omega$ and $R_t = 993\ \Omega$ are known from the experimental procedure. Similarly, the resistances of the Wheatstone bridge can easily be estimated because the top-left resistance $R_{\text{top}} = nR^*$ and the bridge ratio m of the anemometers are specified by the manufacturer (DISA: $R_{\text{top}} = 50\ \Omega$, $m = 20$; StreamLine: $R_{\text{top}} = 20\ \Omega$, $m = 20$; Mini-CTA: $R_{\text{top}} = 20\ \Omega, m = 20$). The choice of wire overheat specifies the value of R^* and thus the value of n. The wire mass m_w can be computed since the wire dimensions and material are known (the tungsten wire nominal diameter is $d_{\text{nom}} = 5\ \mu\text{m}$ but independent measurements estimate its true diameter at $d = 5.5\ \mu\text{m}$), and the parameters c_w and χ can be obtained from the materials tables [1]. We obtain $m_w = 5.5 \times 10^{-10}$ kg, $c_w = 140\ \text{J kg}^{-1}\text{K}^{-1}$ and $\chi = 3.6 \times 10^{-3}\ \text{K}^{-1}$.

The amplifier parameters G, M' and M'' are not provided by the manufacturer and cannot easily be measured on a commercial unit. Similarly, the parameters M_B and E_b are unknown and depend on the actual tuning of the anemometers. We propose the following procedure to estimate these five parameters.

Table 1. Summary of CTA parameters.

	DISA	StreamLine	Mini-CTA
f_{cut}	50 kHz	55 kHz	20 kHz
M	7.20×10^{-3} s	4.10×10^{-3} s	4.10×10^{-3} s
$\mathcal{M}_w$	5.60×10^{-4} s	5.60×10^{-4} s	5.60×10^{-4} s
G	1000	1000	1000
M'	4.23×10^{-6} s	4.86×10^{-6} s	2.22×10^{-5} s
M''	4.48×10^{-12} s^2	5.91×10^{-12} s^2	1.23×10^{-10} s^2
R^*	5.76 Ω	5.76 Ω	5.76 Ω
n	8.68	3.47	3.47
γ	0.645	0.742	0.742
E_0	4.18 V	1.99 V	1.99 V
$M_{B,opt}$	1.42×10^{-9} s	7.85×10^{-10} s	-8.55×10^{-9} s
$E_{b,opt}$	3.68 V	2.80 V	7.66 V

According to Freymuth [9], when a CTA is optimally tuned, its cut-off frequency f_{cut} is related to the wire and amplifier characteristics by

$$f_{cut} = \frac{1}{2\pi\,(MM''/G)^{1/3}}, \tag{4}$$

where the wire time constant M reads

$$M = \frac{1}{2}\frac{[(n+1)R^* + r_L]^2}{nR^*}\frac{1}{R^* - R_a}\frac{m_w c_w}{\chi R_0}\frac{1}{f(U)}. \tag{5}$$

The wire time constant M can be computed using the wire parameters described above. Assuming a typical value of $G = 1000$ for the amplifier gain, the second-order time constant M'' can thus be obtained from equation (4) when the cut-off frequency is known. We furthermore assume, following Freymuth [15], that the second-order amplifier is a sequence of two identical first-order amplifiers. Thus, M' can be obtained as $M' = 2\sqrt{M''}$.

Once G, M' and M'' are known for each CTA, the two remaining parameters E_b and M_B can be obtained if we assume that the CTA is optimally adjusted for a maximally flat frequency response. In this case, Freymuth [9] showed that $M_{B,opt}$ and $E_{b,opt}$ can be expressed as

$$M_{b,opt} = \frac{M'}{G} + \gamma\frac{M''}{G}\frac{1}{\mathcal{M}_w} - \frac{2}{M}\left(\frac{MM''}{G}\right)^{2/3} \tag{6}$$

and

$$E_{b,opt} = \left[2\frac{G}{M}\left(\frac{MM''}{G}\right)^{1/3} - \gamma\frac{M' - GM_{b,opt}}{\mathcal{M}_w}\right]E_0. \tag{7}$$

In equations (6) and (7), the parameters $\mathcal{M}_w$, γ and E_0 are given by [9]

$$\mathcal{M}_w = \frac{m_w c_w}{\chi R_0}\frac{1}{f(U)}, \tag{8}$$

$$\gamma = 1 - \frac{(n-1)R^* + r_L}{(n+1)R^* + r_L}\frac{R^* - R_a}{R^*}, \tag{9}$$

$$E_0 = [(n+1)R^* + r_L]\left(f(U)\frac{R^* - R_a}{R^*}\right)^{1/2}. \tag{10}$$

A summary of the parameters estimated with this procedure is presented in table 1. It was verified that a change of the value of the amplifier gain has negligible effects on the results that will be presented below as long as $G > 500$, which legitimates the assumption of $G = 1000$. Furthermore, it should be emphasized that the procedure assumes that the CTAs are optimally adjusted according to case (3) of Freymuth [9], which implies a flat frequency response below the cut-off frequency. As demonstrated in section 3, only the DISA 55M10 could be optimally adjusted with the available electronic adjustments. The StreamLine and Mini-CTA, while close to the optimum, do not demonstrate a fully flat amplitude transfer function, which leads to a larger uncertainty in the estimation of parameters M_B and E_b than in the case of the DISA 55M10.

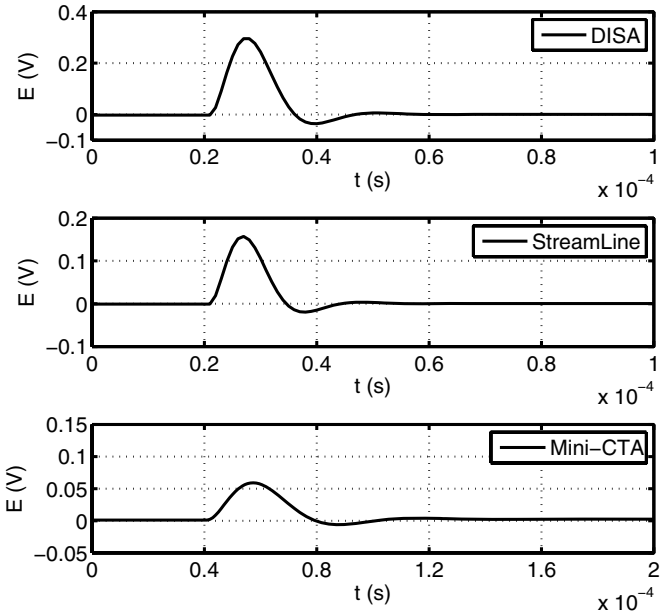

Figure 4. Simulated square-wave responses of the CTAs. Note the different time scales.

The simulated square-wave responses of all three anemometers are presented in figure 4. They were obtained by numerically solving equations (1)–(3) with a square-wave forcing function of amplitude $E_t = 25$ mV. Each signal has the qualitative form expected for a well-tuned anemometer and resembles its experimental counterpart presented in figure 2. The amplitude transfer functions obtained from these simulated pulses are presented in figure 5. In the case of the DISA 55M10, the simulated transfer function is very close to the experimental one presented in figure 3. This good comparison serves as a validation of the procedure that was used to estimate the circuit parameters for this CTA. On the other hand, there are significant differences between the experimental and simulated transfer functions of the StreamLine and Mini-CTA systems. As mentioned in section 3, these two anemometers could not be optimized for a flat frequency response with the available adjustable circuit parameters. Since the estimation procedure for the internal CTA parameters relies on the hypothesis of a perfectly tuned anemometer, it is not surprising that the simulation delivers a flat frequency response, while the actual testing did not. Nevertheless, the simulated square-wave responses and amplitude transfer functions are reasonably close to their experimental counterparts and confirm that Freymuth's model

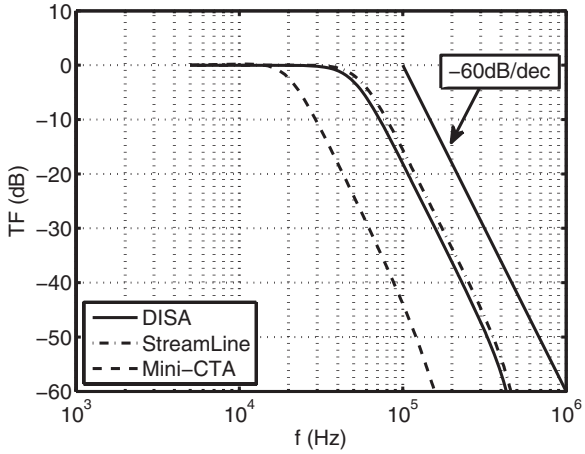

Figure 5. Amplitude transfer function of the simulated CTA models.

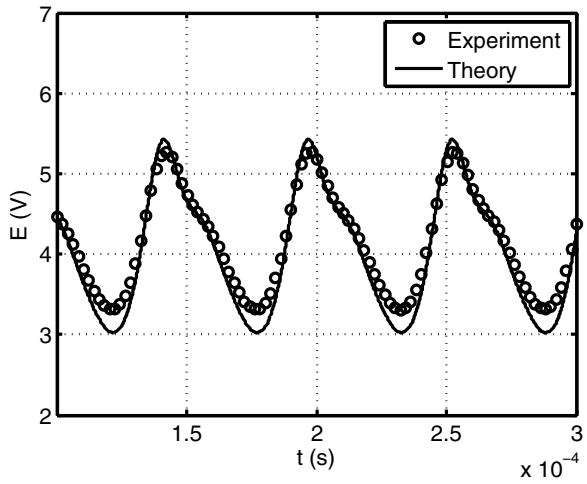

Figure 6. Response of the DISA 55M10 to a sinusoidal perturbation of amplitude $A_t = 200$ mV and frequency $f_t = 18$ kHz.

[9] correctly represents the behavior of commercially available CTAs in the linear range.

4.2. Demonstration of nonlinear behavior

To demonstrate the nonlinearity of the CTA circuits, a sinusoidal perturbation $E_t(t) = A_t \sin(2\pi f_t t)$ is injected in the Wheatstone bridge of the DISA 55M10 anemometer and its output voltage $E(t)$ is measured. In parallel, equations (1)–(3) are solved for the same perturbation signal using the parameters estimated by the method of section 4.1.

Experimental and theoretical output signals of the DISA 55M10 unit for a perturbation of amplitude $A_t = 200$ mV and frequency $f_t = 18$ kHz are presented in figure 6. If the CTA were a linear instrument, the output signal would be a sine wave. Instead, the output signal is significantly deformed, which demonstrates the creation of harmonics by the CTA. The theoretical and experimental results are very close, thus demonstrating the validity of equations (1)–(3) and the estimation procedure described above for the CTA parameters. A similar result, this time obtained with a perturbation frequency $f_t = 27$ kHz, is presented in figure 7. It can be observed that the shape of the output signal is different

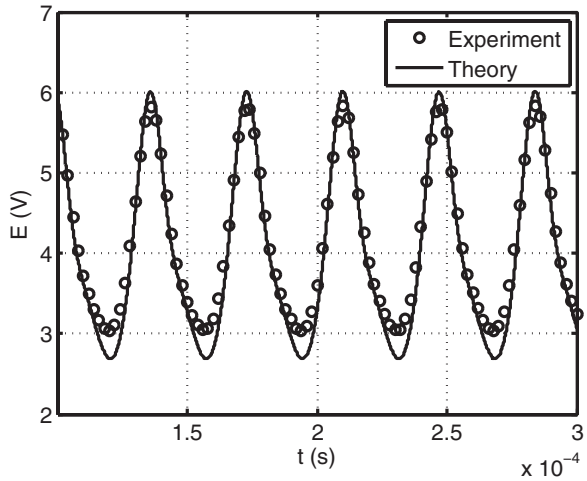

Figure 7. Response of the DISA 55M10 to a sinusoidal perturbation of amplitude $A_t = 200$ mV and frequency $f_t = 27$ kHz.

from that for $f_t = 18$ kHz. This shows that the nonlinear effects induced by the hot-wire and electronic CTA circuit depend on the perturbation frequency, which is consistent with the theoretical results of Freymuth [11, 13]. Again, both theoretical and experimental results are very close.

4.3. Output skewness

In order to investigate the validity of the theoretical CTA model described in section 2 for different amplitudes and excitation frequencies, we compute the skewness factor of the CTA output $E(t)$ for a sinusoidal perturbation $E_t(t) = A_t \sin(2\pi f_t t)$ of varying amplitude and frequency. The skewness factor is computed as $\overline{e^3}/(\overline{e^2})^{3/2}$, where $e = E(t) - \bar{E}$. Three perturbation amplitudes are chosen for the DISA 55M10 anemometer: $A_t = 50$ mV, $A_t = 100$ mV and $A_t = 200$ mV. These perturbation amplitudes correspond to a simulated turbulence level comprised between 0% and 100% depending on the frequency (the simulated turbulence level $u_{\mathrm{RMS}}/\bar{U}$ is estimated by recalling that for a CTA, $e_{\mathrm{RMS}}/\bar{E} = S_U^{\mathrm{CTA}} \times u_{\mathrm{RMS}}/\bar{U}$, where $S_U^{\mathrm{CTA}} \approx 0.25$ is the CTA dimensionless sensitivity to velocity fluctuations [1]). For the StreamLine and Mini-CTA, because of the lower value of the top-left resistance in the Wheatstone bridge, which implies a lower value of the mean output voltage $\bar{E}$ and thus a larger simulated turbulence level, only the two lower amplitudes are used ($A_t = 50$ mV and $A_t = 100$ mV).

The skewness factor simulated and measured on the DISA 55M10 anemometer is presented in figure 8 as a function of the excitation frequency. Its value is strongly dependent on the excitation amplitude and frequency. If the CTA were a linear instrument, the skewness would be exactly zero regardless of the excitation frequency. Instead, for $A_t = 200$ mV and $f_t = 25$ kHz, which correspond to a turbulence level of 35% at half the cut-off frequency of the anemometer, the maximum skewness is about 0.2, in good agreement with Freymuth's earlier findings [11]. This clearly demonstrates the nonlinearity of the CTA governing equations, which agree very well with the experimental results.

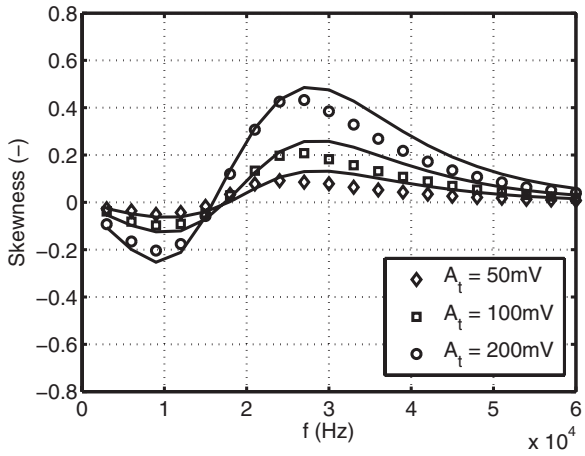

Figure 8. Skewness factor, DISA 55M10. Symbols: experiments; solid lines: theory.

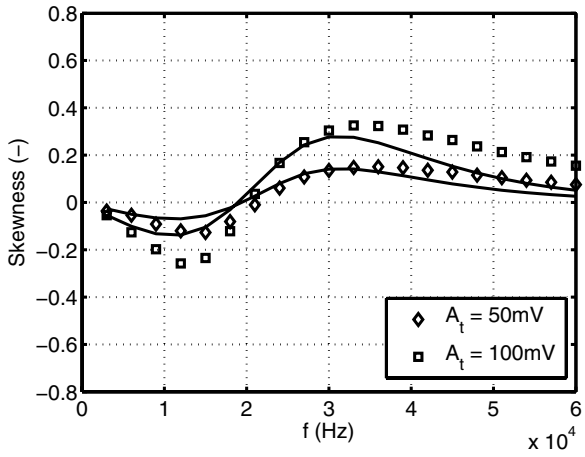

Figure 9. Skewness factor, StreamLine. Symbols: experiments; solid lines: theory.

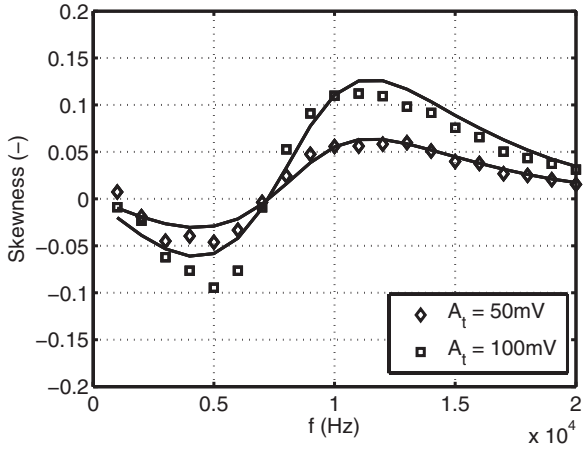

Figure 10. Skewness factor, Mini-CTA. Symbols: experiments; solid lines: theory.

The skewness factors simulated and measured on the StreamLine and Mini-CTA systems are presented in figures 9 and 10, respectively. The values obtained with the StreamLine are similar to those obtained with the DISA 55M10. The maximum skewness factor obtained with the Mini-CTA is lower than for the other two anemometers. This simply reflects the lower frequencies associated with the Mini-CTA, which has a cut-off frequency of 20 kHz compared to 50 kHz and 55 kHz for the 55M10 and the StreamLine, respectively. The level of agreement between theory and experiments is the lowest for the StreamLine system. This is probably caused by the imperfect estimation of its circuit parameters. Indeed, the amplitude transfer function measured on the StreamLine (figure 3) is the furthest away from its theoretical counterpart (figure 5). Nevertheless, the general agreement between skewness factors simulated and measured on the actual anemometers is a clear demonstration that the CTA model described by equations (1)–(3) correctly represents the behavior of commercial CTA systems in the nonlinear range.

5. Conclusion

The results presented above clearly demonstrate that the theoretical CTA model (equations (1)–(3)) originally developed by Freymuth correctly represents the nonlinear behavior of the three commercial CTAs tested in this work. Freymuth's model and results [11, 13] can thus be used with confidence to assess the impact of nonlinearities on measurements of the third-order turbulence moment. Indeed, significant errors occur for large-amplitude velocity fluctuations at frequencies that are not negligibly small compared to the CTA cut-off frequency.

A natural extension of this work would be to use the theoretical CTA model to correct for all nonlinear effects. In theory, a post-processing methodology similar to the one proposed by Berson *et al* [6] for the case of a CVA could be devised. From the measured output voltage $E(t)$, equations (2), (1) and (3) could be inverted sequentially to recover the flow velocity U. This way, all harmonics created by the nonlinear equations would be canceled out, and the true velocity signal $U(t)$ would be obtained.

Exploratory investigations by the authors revealed a number of practical issues that have so far prevented the successful development of such a strategy. The major issue seems to be the large uncertainty in accurately estimating all derivatives required by the inversion procedure from the turbulent signal. Further work along these lines is necessary before a full correction method can be proposed for CTAs.

Acknowledgments

The authors are very grateful to Emmanuel Jondeau for his help in the experimental part of this work. Part of this project was financed by the Samuel-De Champlain program established between the ministère des Relations internationales du Québec and the ministère des Affaires étrangères et européennes de la République française, 63rd session of the Commission permanente de coopération franco-québécoise.

References

[1] Comte-Bellot G 2007 Thermal anemometry *Handbook of Experimental Fluid Mechanics* ed C Tropea, A L Yarin and J F Foss (Berlin: Springer) pp 229–83

[2] Hinze J O 1975 *Turbulence* 2nd edn (New York: McGraw Hill)
[3] Bruun H H 1995 *Hot-Wire Anemometry: Principles and Signal Analysis* (Oxford: Oxford University Press)
[4] Corrsin S 1963 Turbulence: experimental methods *Handbuch der Physik* vol VIII/2 ed S Flügge (Berlin: Springer) pp 524–90
[5] Comte-Bellot G and Schon J-P 1969 Harmoniques créés par excitation paramétrique dans les anémomètres à fil chaud à intensité constante *Int. J. Heat Mass Transfer* **12** 1661–7
[6] Berson A, Blanc-Benon P and Comte-Bellot G 2009 A strategy to eliminate all nonlinear effects in constant-voltage hot-wire anemometry *Rev. Sci. Instrum.* **80** 045102
[7] Freymuth P 1997 Second or third order control theory for constant-temperature hot-wire anemometers? *Exp. Fluids* **23** 175–6
[8] Freymuth P 1998 On higher order dynamics of constant-temperature hot-wire anemometers *Meas. Sci. Technol.* **9** 534–5
[9] Freymuth P 1977 Frequency response and electronic testing for constant-temperature hot-wire anemometers *J. Phys. E: Sci. Instrum.* **10** 705–10
[10] Freymuth P 1969 Nonlinear control theory for constant-temperature hot-wire anemometers *Rev. Sci. Instrum.* **40** 258–62
[11] Freymuth P 1977 Further investigation of the nonlinear theory for constant-temperature hot-wire anemometers *J. Phys. E: Sci. Instrum.* **10** 710–3
[12] Perry A E 1982 *Hot-Wire Anemometry* (Oxford: Oxford University Press)
[13] Weiss J, Berson A and Comte-Bellot G 2011 Nonlinear effects in constant temperature anemometers *Proc. CASI AERO 2011 Conf.* (Montréal: Canadian Aeronautics and Space Institute)
[14] Weiss J, Knauss H and Wagner S 2001 Method for the determination of frequency response and signal to noise for constant-temperature hot-wire anemometers *Rev. Sci. Instrum.* **72** 1904–9
[15] Freymuth P 1997 Interpretations in the control theory of thermal anemometers *Meas. Sci. Technol.* **8** 174–7